IEEE Access
Multidisciplinary | Rapid Review | Open Access Journal

Received 27 October 2023, accepted 8 November 2023, date of publication 16 November 2023,
date of current version 22 November 2023.

Digital Object Identifier 10.1109/ACCESS.2023.3333664

RESEARCH ARTICLE

Deterministic Chaotic Propagation Model

ALBERTO LEONARDO PENTEADO BOTELHO[1,2], CRISTIANO AKAMINE[2], AND PAULO BATISTA LOPES[2]

[1]LM Telecomunicações, São Paulo 01333-908, Brazil
[2]Graduate Program in Electrical Engineering and Computing, Universidade Presbiteriana Mackenzie, São Paulo 01333-908, Brazil

Corresponding author: Alberto Leonardo Penteado Botelho (abotelho@lmtelecom.com.br)

This work was supported in part by the LM Telecomunicações Ltda., and in part by the Coordination for the Improvement of Higher Education Personnel (CAPES - Fundação Coordenação de Aperfeiçoamento de Pessoal de Nível Superior).

ABSTRACT Coverage prediction is an essential method of planning broadcast and long-range wireless communication systems, minimizing the need for field measurements to adjust the coverage area and consequently reducing the time and cost of implementation. Coverage prediction methods use statistical simplifications in conjunction to uncertainty quantification algorithms to assist in modeling multipath effects and impulsive noise, notably hard to be statistically considered. This paper presents a new approach to represent electromagnetic wave propagation uncertainties based on chaotic dynamical systems to model the behavior of multipath effect and impulsive noise. A novel Deterministic Chaotic Propagation Model (DCPM) is presented and used to predict coverage area in a DVB-T2 broadcast system in diverse transmission environments. The results indicate that the predicted area of bad reception is smaller in comparison to the one obtained using traditional methods. Therefore, fewer signal repeaters can be used to provide good TV reception in this area, causing a significant cost reduction in the set-up of a broadcast system. Another parameter used to evaluate the quality of reception is the carrier to noise power ratio (C/N) threshold for a bit error rate (BER) of 10-7. The DCPM indicate a C/N threshold equal to 13.7 dB in dense urban environment and 13.4 dB in rural environment using a moderately less robust modulation configuration. Employing a more robust configuration, the C/N threshold is equal to 0.9 dB in all environments. These numbers match the obtained by the traditional propagation models.

INDEX TERMS Broadcast, chaotic dynamical systems, Doppler effect, impulsive noise, long-range wireless communication, multipath, propagation.

I. INTRODUCTION

In broadcasting and long-range wireless communication systems, the electromagnetic wave must reach the receiver with a minimum intensity to make it possible to decode the signal without errors. The main influences on the signal intensity in the receiver are the power radiated by azimuth, angle of arrival, scattering, power dissipation, multipath, additive Gaussian noise and impulsive additive noise [1].

The main causes of uncertainty are the difficulty in representing multipath and impulsive noise because these two effects have unpredictable behavior, hard to be statistically modeled. The influence of multipath depends on the severity of obstructions by buildings and natural obstacles. The influence of impulsive noise depends on the reception environment [2], [3].

Due to the complexity of representing all elements of Nature, a reliable coverage prediction is necessary to minimize the field measurements to adjust the coverage area and consequently reduce the time and cost of planning a communication system. Propagation models are available in the literature and are a statistical simplification that considers the main elements of Nature [2]. Statistical simplification can be minimized with uncertainty quantification algorithms, such as the Monte Carlo method, where lower probability areas are considered uncertain and eligible for field measurement and coverage adjustment [4].

This paper presents a new concept to represent electromagnetic wave propagation uncertainties with the application of chaotic dynamical systems, notably multipath and impulsive

The associate editor coordinating the review of this manuscript and approving it for publication was Yafei Hou.

noise. The propagation effects are divided into additive Gaussian noise, chaotic static multipath, chaotic Doppler Effect and chaotic impulsive noise. The sum of propagation effects is called in this paper as the Deterministic Chaotic Propagation Model (DCPM).

The model identifies the reception threshold of the communication system in the best situation under the effect of AWGN (Additive White Gaussian Noise) and in the worst situation under the effect of multipath and impulsive noise typical of rural, hilly rural, urban and dense urban environments. The uncertainty areas considerably decrease when considering the threshold difference between the best and worst situations. The model was tested on the DVB-T2 (Second Generation the Terrestrial Digital Video Broadcasting) because it is widely spread around the globe and because its technical features are the basis of technological evolutions of the most recent digital TV standards. The entire encoding and decoding process was adapted for software simulation and identified the reception threshold in different configurations [5].

The literature presents chaotic signals applications in telecommunications systems. The main proposals revolve around the transmission of a digital signal encoded in a chaotic signal. It was demonstrated that chaos-based modulation techniques make the interception and decoding of Power Line Communication (PLC) system data more difficult for an eavesdropper [6], [7].

In the wireless communications, the literature presents hypotheses that the propagation behavior is closer to the deterministic chaotic. Alternative models to the Monte Carlo were proposed, such as the Monte Carlo hybrid system with chaotic polynomial, with aim of achieve a fast convergence [8] and the chaotic polynomial system, to derive mean and variance of an electromagnetic distribution, useful in cases of numerical simulations where a transfer function of a channel or the radius is not provided analytically [9]. Initiatives based on deterministic chaotic equations have been proposed to adjust statistical errors in the propagation model and represent the resulting waveform closer to that found in Nature [10]. A multipath propagation model was proposed in a Jakes model extension, with the chaotic Lorenz attractor application [11]. Chaotic impulsive noise generators were modeled so that power, duration and spacing of the pulses have indeterminate characteristics, closer to the behavior found in nature [12]. This study introduces a novel approach to the use of chaotic dynamical systems to model the unpredictable propagation impairments as well as perform coverage analysis of a broadcast transmission to foresee the strength of the signal in given geographic area. The three main contributions of this article may be summarized as follows.

- Develop a modeling of propagation effects closer to the unpredictable behavior of multipath and impulsive noise found in real broadcasting and long-range wireless communication environments.

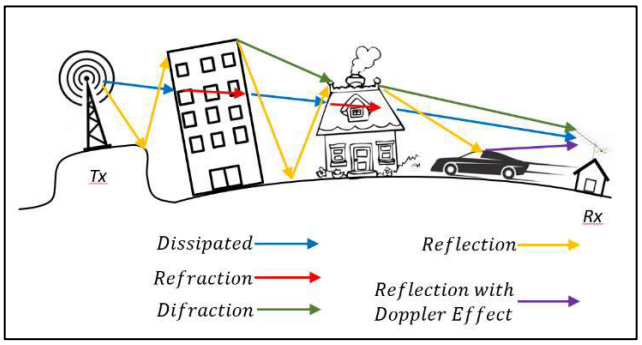

FIGURE 1. Typical multipath situation.

- Minimize the propagation models uncertainties, and consequently reduce the time and cost of designing a communication system.
- Simulate the robustness of the communication system for different propagation environments.

This paper is organized as follows. In section II, the concept of multipath, stochastic and deterministic tools to calculate multipath and mitigation methods are presented. Then, in section III, the concept of additive noise is presented as well as stochastic and deterministic tools to calculate additive noise, in particular impulsive noise and mitigation methods. Section IV covers the concept of chaotic dynamical system, the tools to generate chaotic signal and the possible methods to model chaotic multipath and chaotic impulsive noise. In section V, the proposal of the chaotic propagation model is presented, and the results are applied to the model of DVB-T2 system. Conclusions of the paper are drawn in the Section VI.

II. MULTIPATH

After converting the energy into an electromagnetic field, the electromagnetic wave is scattered in all directions in space and dissipated by the transmission medium. When the electromagnetic wave hits an obstacle in its path, a part of the energy of the wave returns by reflection, a second part continues to be transferred by refraction, possibly in an altered direction, and a third part of the wave is scatter by diffraction, going around the obstacle. The movement of the receiver or the obstacle shifts the frequency by the Doppler Effect. The combination of direct, reflected, refracted, diffracted and Doppler Effect is called multipath [1]. Fig. 1 shows a typical multipath situation, where Tx (transmitter) radiates the transmitted signal to the Rx (receiver), under multipath effect, due to the obstacles found in an urban environment.

A simple receiver does not distinguish the different components of the multipath and attempts to recover the sent information based on the summation of the received waves. In harsh situations, without any measurement precaution, the accumulated errors cannot be eliminated and are known as irreducible errors [3].

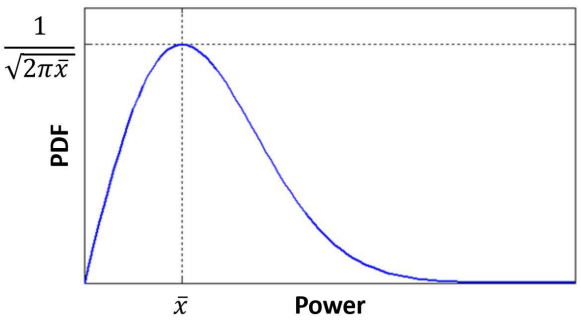

FIGURE 2. Rayleigh PDF.

A. PROPAGATION MODELS

Propagation model is a tool that describes how the signal is radiated from the transmitter to the receiver to predict the power strength throughout the service area [2]. The representation of the coverage area by the propagation model is a statistical simplification that can correspond to the propagation pattern, considering multiple delayed waves scattered at different paths [11].

By making reliable coverage predictions, the need for field measurements to adjust the coverage area is considerably reduced, also implying a reduction in project time and cost. Propagation models do not always provide accurate predictions. The prediction error varies due to the environmental peculiarity of each location [13].

Techniques to minimize errors in propagation models have been widely used. As an example, the Monte Carlo method performs summation of signals in a log-normal distribution to quantify the uncertainties of propagation models [4].

B. STOCHASTIC MULTIPATH MODELS

The multipath effects in the channel can be simulated by stochastic models, which do not try to predict the impulse response, but rather to predict the probability distribution function (PDF) over a large area and are more used in systems comparison [3], [14].

The literature provides different distributions to represent the multipath found in the medium, such as Rayleigh, Rician and Nakagami. Rayleigh applies the Central Limit Theorem, where each path of the multipath can be modeled as circularly symmetric, gaussian, time-varying and has been shown to be best suited for applications with large numbers of multipaths [15].

Fig. 2 shows the Rayleigh PDF. The PDF axis describes the probability of a given power reaching the receiver, which assumes always positive values, with the integral of the PDF over the entire space always equal to 1. The Power axis describes the range of power values. $\bar{x}$ is defined as the time average of the power.

C. DETERMINISTIC MULTIPATH MODELS

Deterministic models are possible, as long as it is obtained precise information on the electromagnetic wave, topology and obstacles, such as spatial distribution, level of reflection, refraction and diffraction, scattering features, terrain roughness, wavelength, angle of arrive, shape and penetration rate in obstacles [16].

Deterministic models are available in the literature, such as the Jakes fading model to simulate time-correlated Rayleigh fading waveforms and the Bhuvaneshwari model to simulate path loss by ray tracing approach for non-line of sight indoor Propagation [11], [17].

Yee proposes reception model obtaining the decision variable, in which involves demodulating each of subcarriers of the received signal defined by (1), where $r(t)$ is the multipath reception model, $a_{Nm}[k]$ represents the transmitted binary signal assumed as equal probability binary antipodal 1 or -1, Nm represents the nth multipath, k represents the nth bit span, N represents parallel copy of the symbol, $p_{(i)}$ is the random amplitude, θ_i is the random phase, n_t is the random AWGN, F is a subcarrier and T_b is the bit period [18].

$$r(t) = \sum_{Nm=0}^{M-1} \sum_{i=0}^{N-1} p_{(i)} c_{(Nm)}[i]\, a_{Nm}[k] \times \cos\left(2\pi f_c t + 2\pi i \frac{F}{T_b} t + \theta_i\right) + n_t \quad (1)$$

In typical broadcast and long-range wireless communication propagation environments, precise electromagnetic wave, topology, and obstacle information is unfeasible, computationally complex, and not treatable with a simple analysis [2], [13], [16]. An alternative to make a deterministic model viable is the use of geographic and morphological information from a database of a given geographic location [3], [14].

The COST 207 project parameterized multipath profiles, considering measurements in several countries on the European continent [19]. The Saleh–Valenzuela model is used as the basis for the extended model. The amplitude of each path is assumed to be a random variable of Rayleigh distribution, whose mean square is described by the double exponential decay. The impulse response of the channel can be expressed by (2) and (3), where $h(t)$ is the impulse response, l is the cluster, k_l is the arrival in the cluster, β_{kl} is the average power of the first arrival of the first cluster and $e^{j\Phi\omega k_l l}$ represents the statistically independent random phase, where $\Phi k_l l$ is uniform at $[0,2\pi]$. T_l is the time of each arrival in the nth cluster, τ_{kl} is the time of each arrival in the nth arrival in the nth cluster, Γ is the cluster decay and γ is the arrival decay. [20].

$$h(t) = \sum_{l=0}^{\infty} \sum_{k_l=0}^{\infty} \beta_{k_l l} e^{j\Phi\omega k_l l}\, \delta(t - T_l - \tau_{kl}) \quad (2)$$

$$\beta_{kl}^2 = \beta^2(T_l, \tau_{kl}) = \beta^2(0,0) e^{T_l/\Gamma} e^{-\tau_{kl}/\gamma} \quad (3)$$

Multipath patterns parameters found in the transmission medium, such as average delay, maximum delay and arrival angle are found in the literature for different propagation environments [21], [22].

Multipath profile does not consider Doppler Effect. Doppler Effect arises when the receiver and/or multipath obstacle is in motion and causes frequency change and the

consequences are spectrum broadening, acousto-optic iteration and Brillouin scattering [1]. In modulations that use multi-carriers, the Doppler Effect causes mismatch between local oscillators for frequency conversions and generates CFO (Carrier Frequency Offset), which is carrier frequency shift, causing intersymbol interference from other carriers that are not orthogonal to the filter [23], [24]. The mean vector error expressed by distance can be calculated in (4), where E_V is the mean vector error expressed by distance, θ represents the angle of the observed vector Φ represents the angle of the error vector and d_i represents the module of the symbol vector with respect to the decision threshold.

$$E_V = \sum_{i=1}^{P} \sum_{j=2}^{Q} d_i[sin\,(\theta - \Phi) + cos\,(\theta - \Phi)] \qquad (4)$$

D. MULTIPATH MITIGATION

Channel estimation is the most important technique to mitigate multipath. Methods based on pilot signals, least square algorithm, and cyclic prefix are commonly used. For estimation purposes, first, channel response at some specific frequencies is obtained by means of the analysis pilot tones that are embedded in the transmitted signal. These responses in specific frequencies are interpolated to provide the overall channel response [25], [26].

Multicarrier based systems use the insertion of guard interval with duration equal to or greater than the prospective maximum delays between received versions of the transmitted signal that arrived at the receiver in different time instances. The guard interval is generally filled with a cyclic prefix, which can be described as a copy of the final part of the useful symbol, in order to guarantee the robustness of the system against inter-symbol and inter-frame interference. After extraction of the cyclic prefix in the receiver, a cyclic periodic convolution of the symbol is obtained, where a complex multiplication of symbols occurs, which allows the removal of the intersymbol interference and interference between frames [27].

After channel estimation, the equalization is performed. This is a technique, in which the combined filter does the convolution of the unknown signal with a conjugate version of the time-inverted delayed signal, and the equalizer compensates for the distortion caused by multipath [28].

In practice, the use of channel estimation and equalizer is unable to achieve perfect performance, resulting in residual intersymbol interference. Residual CFO still destroys the orthogonality of the received signal, worsening the symbol error rate SER (Symbol Error Rate) [25], [28]. In the residual CFO, the spacing of the subcarriers can vary from small (0.005), medium (0.01) and large (0.015) which rotates the vector by 0.0314, 0.0628 and 0.0942 radians respectively [29], [30].

Channel coding contributes to data reception in a digital communication system. This technique is used to identify and recover a certain amount of corrupted data without retransmitting the information. Error-correcting codes can correct a limited number of errors. Byte interleaved spreads burst errors in the time domain, increasing error detection and correction capabilities [31].

III. ADDITIVE NOISE

Additive noise is an unwanted impairment that degrades the electromagnetic wave. It may be generated by external sources or by the transmission and reception system itself. The receiver can decode the transmitted signal without errors if the electromagnetic wave has a C/N (Carrier-to-Noise Ratio) equal to or greater than its reception threshold. C/N compares the received signal strength "C" with the noise strength "N". The higher the C/N, the smaller the noise effect [32].

AWGN is a simple mathematical model of noise that corrupts the electromagnetic wave in the whole band with constant spectral density expressed in Watts per Hertz and with Gaussian distribution. AWGN does not explain the phenomena of fading, frequency selectivity, interference, non-linearity, dispersion or multipath, but it is useful to simulate the basic behavior of a system before the effect of random processes that occur in Nature [33].

An important source of electromagnetic wave degradation is the man-made noise that appears in urban environments, created by the electric start of cars, power lines, electrical current switches, arc welders and fluorescent lights, among others. This phenomenon is known as impulsive noise and appears as a random sequence of pulses and cannot be associated with a probabilistic distribution [34]. It can be divided into Class A, Class B or Class C. Class A has coherent transients at the receiver, with constant phase differences, possibly with overlapping waves and are irrelevant in the impact of the communication system. Class B is incoherent, composed of short impulses with a predominance of transient decays and is relevant in the impact of the communication system. Class C is the sum of Class A and Class B components [32].

A. STOCHASTIC IMPULSIVE NOISE MODELS

To develop a stochastic model of impulsive noise, PDF of power, duration and spacing between arrivals are essential. Impulsive noise can follow particular distributions if the source is known. Comparing impulsive noise samples with distribution models found in the literature, it is verified that none of the statistical distributions can represent impulsive noise [34].

Middleton's stochastic model for Class A phenomena considers noise bandwidth compared to receiver bandwidth [32]. The symmetric alpha-stable stochastic model for Class B can also be used for statistical modeling of impulsive noise through its characteristic functions [35]. The Ghosh model demonstrates equivalence between the Bernoulli and Gauss model of impulsive noise in the discrete-time domain and the continuous-time Poisson model. All random sequences are assumed to be independent of each other and therefore, each data symbol is transmitted independently [36]. The

TABLE 1. Impulsive noise coefficients.

Environment	g	h	m	n
City Center	79.3	32.9	106.5	32.4
Factory Estate	96.8	40.8	116.3	35.6
Business Centre	56.6	32.6	50.8	11.5
Suburban	45.9	21.9	126.9	41.0
Rural	104.1	53.3	130.4	51.2
Quiet Rural	65.7	39.3	100.9	45.6
Road Junction	69.8	34.3	128.8	40.8
Railway	91.4	39.3	142.0	44.8

TABLE 2. Impulse noise statistics in urban environment for horizontal polarization.

Environment		Quiet	Noisy
Power (μW)	Average	0.43	1.71
	Standard Deviation	0.97	9.03
Duration (μs)	Average	0.23	0.16
	Standard Deviation	0.23	0.21
Spacing (μs)	Average	54.16	48.78
	Standard Deviation	36.12	39.43

Fernández model was presented in the studies of the DTG II work team, led by the research and development area of the British Broadcasting Corporation (BBC), and is based on theoretical and practical studies, with the main objective of obtaining a set of waveforms and methods that could faithfully represent the effects of impulsive noise for digital television [37].

B. DETERMINISTIC IMPULSIVE NOISE MODELS

Physical impulsive noise generators can be used to test the robustness of the telecommunications system. The impulsive noise generator should allow control over the parameters and reproducibility in any environment with a window of programmable pulses in the time domain [38].

Wagstaff and Merricks carried out measurements in a voltage density field of Class B impulsive noise in different environments and frequencies, whose average is summarized in (5), standard deviation is summarized in (6) and coefficients is summarized in Table 1, where M_{in} is the average power density of impulsive noise, σ_{in} is the standard deviation of impulsive noise and f is the frequency (MHz) [39].

$$M_{in} = g - hlog(f) \tag{5}$$

$$\sigma_{in} = m - nlog(f) \tag{6}$$

Artificial noise levels in the VHF and UHF band are documented by the International Telecommunication Union Recommendation ITU-R P.372-7, based on research from the 1970s. Average values from current studies appear significantly higher, indicating the possibility that the number of electronic devices might have increased [39], [40]. Table 2 summarizes the duration and standard deviation of impulsive noise, for horizontal polarization, in a quiet and noisy urban environment, at the frequency of 762 MHz, concluding that the pulses in a quiet environment have shorter duration, lower amplitude and greater distance between pulses when compared to a noisy environment [34].

C. IMPULSIVE NOISE MITIGATION

As with the multipath, channel coding is a technique used to identify and recover a certain amount of corrupted data without the need to retransmit the information. However, in modulations that use multiple carriers, a single noise peak, present only in a sample of a single symbol, spreads to all subsymbols, due to the processing of the FFT (Fast Fourier Transform). FFT is ideal in AWGN situation and impulsive noise may cause an error to all of them if their power peak is high enough and consequently the detection and correction mechanisms lose their effectiveness [41].

Impulsive noise suppression algorithms are available in the literature and aim to detect the presence of a predetermined high amplitude pulse, remove its energy and replace it with zero. These impulsive noise detection techniques are limited and partially efficient [42]. Maximum likelihood detection algorithms can be applied to the receiver vector. The resultant is processed by the threshold detector to estimate the complex amplitudes at the impulsive noise positions and can be expressed by (7), where n_w^i is the maximum likelihood detector, T represents the threshold, w represents the first mapped detector and i represents the nth iteration of the algorithm [43].

$$n_k^i = \begin{cases} 0 & for \left|n_w^i\right| \leq T \\ \left|n_w^i\right| & for \left|n_w^i\right| > T \end{cases} \tag{7}$$

IV. CHAOTIC MULTIPATH AND IMPULSIVE NOISE

Although the multipath is widely simulated with stochastic models, the literature presents hypotheses that its behavior is closer to the deterministic chaotic one. Initiatives based on deterministic chaotic equations have been proposed to adjust statistical errors and represent the resulting waveform closer to that found in Nature [10], [11].

Impulsive noise is a challenge to be modeled due to the characteristic of unpredictability in the intensity, duration and spacing of the pulses. Chaotic impulsive noise generators have indeterminate characteristics, closer to the multipath and impulsive noise behavior [12].

A dynamic system can be described as a set of possible previous states that determine the present state. The dynamic system can exhibit periodic, or aperiodic behavior [44]. The definition of chaotic signal can be simplified as a signal limited in amplitude, aperiodic and presents sensitive dependence with the initial conditions [45], or it can be defined as dense periodic states in the invariant set and topologically transitive [46].

Discrete dynamic system is described in the literature by means of maps. Maps with different characteristics can be used as chaotic signal generators [45].

One-dimensional maps have iterations belonging to a space of real numbers, so they can be applied in

telecommunications with a number of samples per second representing the bit rate of a real communication system [47]. Tent map is an example of a one-dimensional map can be defined by (8) and (9), where $s(n+1)$ represents the next state of the dynamical system, $s(n)$ is a sample process function and $f_T(s)$ is the tent map function [48].

$$s\,(n+1) = f_T\,(s\,(n)) \tag{8}$$

$$f_T\,(s) = 1 - 2\,|s| \tag{9}$$

Chaotic systems with strange attractors are characterized by trajectories confined in a region limited in space and phase, flattening the curve in one of the horizontal or vertical directions and stretching in the other, being bent and reinjected into the system. The various directions form the multidimensional map, with transients that never decay, with orbits that shuffle endlessly without settling down [47]. Hénon map is an example of a bi-dimensional map and can be defined by (10), where $H_{(n+1)}$ represents the next state of the Henon map, $x_{(n)}$ is the current state of the x axis $x_{(n+1)}$ is the next state of the x axis $y_{(n+1)}$ is the next state of the y axis and a and b are real variables. For $a = 1.4$ and $b = 0.3$ [49].

$$H_{(n+1)} = fx_{(n)} = \begin{pmatrix} x_{(n+1)} \\ y_{(n+1)} \end{pmatrix} = \begin{pmatrix} y_{(n)} + 1 - ax_{(n)}^2 \\ bx_{(n)} \end{pmatrix} \tag{10}$$

It is possible to combine a software-implemented graphical interface with deterministic chaotic models. Stochastic propagation models, such as AWGN, Rayleigh and Rician can be replaced by a new model that represents all stages of propagation in a deterministic way, with the aim of increasing the efficiency of the propagation model and being an alternative to quantify uncertainties [3].

This project proposes that propagation effects are divided into Gaussian additive noise, chaotic static multipath, chaotic Doppler effect and chaotic impulsive noise. Additive Gaussian noise can be represented by the AWGN stochastic distribution. Static multipath, Doppler effect and impulsive noise have irregular and unpredictable behavior, so a deterministic model based on chaotic dynamical systems is proposed.

A. CHAOTIC STATIC MULTIPATH

To model chaotic static multipath, a block was developed to divide the main signal into 12 versions, to simulate 12 paths. 1 path with the leading symbol and a sequence of 11 paths with delayed symbols, as recommended by [19].

The maximum delay was defined as more recent measurements by Jeong, et. al. In a rural environment, it is considered a maximum delay of 5.9 μs, referring to measurements in a rural location. In a hilly rural environment, it is considered 7.1 μs, referring to measurements in a mountainous location. In an urban environment, it is considered 6.2 μs, referring to urban measurements with a predominance of roofs. In a dense urban environment, it is considered 7.5 μs, referring to urban measurements with a predominance of skyscrapers [22].

The decay of delays was based on the extended Saleh–Valenzuela model, which was added to a chaotic function, configured to be contained in the maximum orbit of 5 dB in accordance with the standard deviation measured by [21].

For the chaotic function, a one-dimensional chaotic generator based on the tent map was developed. The one-dimensional map has iterations belonging to a space of real numbers, so a fixed chaotic value was assigned to each route, simulating a fixed obstacle [49].

The chaotic static multipath can be summarized in (11), (12), (13) and (14), where $N_{CE\circledast}(i)$ is the chaotic static multipath noisy bitstream, F_B is the bitstream, i is the nth iteration of the algorithm, M_{pE} is the static multipath, NP is the nth path from 2 to 12, P_1 is the main path vector position, P_{NP} is the nth delay vector position, D_{NP} is the nth path decay adapted from the Saleh–Valenzuela model, $\circledast_{tentNP}$ is the nth iteration of the one-dimensional chaotic signal generator, tent map, I_{ca} is the delay suppression index and x_0 is the initial condition.

$$N_{CE\circledast}(i) = {}^{F_B}/_{M_{pE}}(i) \tag{11}$$

$$M_{pE} = P_1 + \sum_{P_{NP}=2}^{12} (P_{NP} * D_{NP} * \circledast_{tentNP} * I_{ca}) \tag{12}$$

$$\circledast_{tentNP}(i) = 1 - 2x_0 \tag{13}$$

$$\circledast_{tentNP}(i+1) = 1 - 2\,\circledast_{tentN}(i) \tag{14}$$

B. CHAOTIC DOPPLER EFFECT

To model chaotic Doppler Effect, a carrier frequency shift block was developed to represent the vector angular error of the CFO, with chaotic variation. To generate the chaotic variation, a two-dimensional chaotic generator, Hénon map, was adapted, which can present a confined orbit in a certain region of space [49].

The transmitted signal enters the in port of the Complex Phase Shift subblock. The X axis of the Henon map, is adjusted to be contained in a predetermined maximum orbit, converted into radians and input from the Phase port of the Complex Phase Shift subblock. Each symbol entering the in port has its phase changed chaotically by the values entering the Ph port.

The maximum angle of variation considered empirical values after the process of channel estimation and equalization. For rural and hilly rural environments, it considered a maximum vector error of 0.0314 radians, referring to measurements of small displacements. For the urban environment, it considered a maximum vector error of 0.0628 radians, referring to measurements of moderate displacements. For the dense urban environment, it considered a maximum vector error of 0.0942 radians, referring to measurements of large displacements [29], [30].

The chaotic Doppler Effect can be summarized in (15), (16) and (17), where θ_{CFO} is the CFO chaotic vector angular error, F_B is the bit stream, i is the nth iteration of the algorithm, ω_c is the carrier angular frequency, Φ is the error

vector angle, and $\circledast_{X_{Hénon}}$ is the X axis of the Henon map, $\circledast_{Y_{Hénon}}$ is the Y axis of the Henon map, $a = 1,4$ and $b = 0.3$.

$$\theta_{CFO} = F_B * \sin\left(\omega_c \pm \Phi * \circledast_{X_{Hénon}}\right) \quad (15)$$

$$\circledast_{X_{Hénon}}(i+1) = 1 + y_i - ax_i^2 \quad (16)$$

$$\circledast_{Y_{Hénon}}(i+1) = by_i \quad (17)$$

C. CHAOTIC IMPULSIVE NOISE

To model chaotic impulsive noise, a noise generator block was developed, where the intensity, duration and spacing have chaotic variation. To generate chaotic variation, two bidimensional chaotic generators Hénon map were adapted, which can present a confined orbit in a certain region of space [49].

In order to make the 2 generators divergent, the first chaotic impulsive noise generator was configured with an initial condition of 0.1 and the second impulsive noise chaotic generator was configured with an initial condition of 0.5.

1 axis of the chaotic signal is adjusted to be contained in the orbit from 0 to 1 and divided into sine and cosine functions and converted into complex Phase and Quadrature values. The resultant is a complex number noise, with constant intensity and chaotically variable angular component.

1 axis of the chaotic signal is adjusted to be contained in the orbit from 0 to 1 and multiplied by the noise generator with chaotic phase. The resultant is complex number noise, with chaotically variable vector position.

For the noise to be impulsively inserted into the system, a switch between chaotic noise and a sequence of zeros was developed. 2 axes of the chaotic signal are summed to have a switch clock function.

The switch decision value was defined according to more recent measurements by Sánchez, et. al. [34]. In a rural and hilly rural environment, it considered an average of 1 pulse every 235 sequences of zeros, referring to measurements in a quiet place. In an urban and dense urban environment, it considered an average of 1 pulse every 157 sequences of zeros, referring to measurements in a noisy place.

The maximum power of chaotic impulsive noise considered the power spectral density measured by Wagstaff and Merricks. Rural and hilly rural environments were set to -43 dBμV/MHz. Urban environment was configured with intensity of -33 dBμV/MHz. Dense urban environment was configured with intensity of -11 dBμV/MHz [39]. In systems that have impulsive noise suppression, the level of suppression must be implemented [43].

The resultant is a chaotic impulsive noise, with chaotic variation of intensity, phase and spacing. The chaotic impulsive noise can be summarized in (18), (19), (20), (21) and (22), where $IN_{\circledast}$ is the chaotic impulsive noise, $N_{QAM\circledast}$ is the complex number chaotic noise, Ω is the switch variable, X_{IQ} is the angular component of the in-phase and quadrature noise, X_I is the in-phase component, X_Q is the quadrature component, ω_c is the angular frequency of the carrier and i is the nth iteration of the algorithm, $\circledast_{X_{Hénon}}$ is the X axis of the Henon map, $\circledast_{Y_{Hénon}}$ is the Y axis of the Henon map, $a = 1,4$ and $b = 0.3$.

$$f\left(IN_{\circledast}\right) = \begin{cases} 0, & \Omega < x \\ N_{QAM}, & \Omega \geq x \end{cases} \quad (18)$$

$$N_{QAM\circledast}(i) = X_{IQ}(i) * \circledast_{X_{Hénon}(i)} \quad (19)$$

$$X_{IQ}(i) = X_I(i)\,cos(\omega_c i) - X_Q(i)\,sin(\omega_c i) \quad (20)$$

$$\circledast_{X_{Hénon}}(i+1) = 1 + y_i - ax_i^2 \quad (21)$$

$$\circledast_{Y_{Hénon}}(i+1) = by_i \quad (22)$$

V. CHAOTIC PROPAGATION MODEL IN THE CHANNEL

The challenge for a broadcasting or long-range wireless communication system is to model the effects of propagation between the transmitter and the receiver as faithfully as possible. The greater the reliability of the modeling, the smaller the need for field measurements to adjust the coverage area, also implying a reduction in project time and cost [2].

The current computational processing capacity allows a communication system to be implemented by software with a graphical interface to simulate the effects of all transmission, channel, and reception stages.

Any communication system can be implemented by software with a graphical interface to simulate all transmission and reception steps. To simulate the noise, Gaussian additive noise was used, added with chaotic static multipath, chaotic Doppler Effect and chaotic impulsive noise, that can be summarized in (23), where N_T is the total noise, N_G is the bit stream with additive Gaussian noise, $N_{CE\circledast}$ is the bit stream with chaotic static multipath noise, $\theta_{CFO}(i)$ is the chaotic vector angular error of the CFO, $IN_{\circledast}$ is chaotic impulsive noise in complex number and i is the nth iteration.

$$N_T(i) = N_G(i) + N_{CE\circledast}(i) + \theta_{CFO}(i) + f\left(IN_{\circledast}\right)(i) \quad (23)$$

A. DVB-T2

The communication system chosen to test the chaotic propagation model in the channel was DVB-T2, because it is a current and widely disseminated second generation digital terrestrial television transmission standard [5].

The DVB consortium has developed the DVB-T2 CSP (DVB-T2 Common Simulation Platform) simulator, which simulates the DVB-T2 standard with the entire transmission and reception chain in open-source Matlab model and published by the BBC [50].

The DVB consortium has a channel model to simulate multipath effects with distributions Gaussian, Ricean, Rayleigh and 0 dB 2-path, at 90% of the guard interval with 1 Hz [51]. The DVB consortium parameterized the minimum C/N for BER of 1.10^{-7} after LDPC with approximate values and considering perfect performance of the channel estimation.

Table 3 shows a comparison of the minimum C/N between the parameterization of the DVB consortium, the DVB-T2 CSP simulator, and the DCPM, in diverse transmission environments, for 8 MHz bandwidth, modulation of 64 QAM, and code-rate of 3/4.

TABLE 3. Threshold C/N between the DVB channel models (8 MHz, 64 QAM, and code-rate of 3/4).

Estocastic environment	DVB guide (dB)	DVB-T2 CSP (dB)	Deterministic environment	DCPM (dB)
Gaussian	13.5	13.3	Rural	13.4
Ricean	13.8	13.7	Hilly Rural	13.4
Echo 0 dB	15.5	15.3	Urban	13.5
Rayleigh	15.6	15.6	Dense Urban	13.7

TABLE 4. Threshold C/N between the DVB channel models (6 MHz, QPSK, and code-rate of 1/2).

Estocastic environment	DVB guide (dB)	DVB-T2 CSP (dB)	Deterministic environment	DCPM (dB)
Gaussian	0.7	0.9	Rural	0.9
Ricean	0.9	1.1	Hilly Rural	0.9
Echo 0 dB	1.6	1.6	Urban	0.9
Rayleigh	2.0	1.9	Dense Urban	0.9

FIGURE 3. Coverage area with Monte Carlo method application.

Table 4 shows a comparison of the minimum C/N between the parameterization of the DVB consortium, the DVB-T2 CSP simulator, and the DCPM, in diverse transmission environments, for 6 MHz bandwidth, modulation of QPSK, and code-rate of 1/2.

DVB-T2 has good robustness to multipath and impulsive noise in all environments studied. In the DVB-T2 case with a less robust configuration, the difference between the simpler rural environment and the complex dense urban environment is 0.3 dB. In the DVB-T2 case with a more robust configuration, there is no difference between the simpler rural environment and the complex dense urban environment.

The results show that for the DVB-T2 case, the difference between the simpler gaussian environment and the complex Rayleigh distribution environment is 2.3 dB in less robust configuration and 1 dB in more robust configuration. The Rayleigh distribution is too pessimistic to represent the real propagation effects.

The subjective comparison of the existing model with the proposed model can be analyzed by coverage prediction software. Fig. 3 shows a hypothetical coverage simulation in the City of Rio de Janeiro, in Brazil. The software used to predict the coverage area was Progira, [52] which operates on the ArcGIS platform, to create and share geographic maps, scenes, applications, layers, analytics, and data [53]. The propagation model used was CRC-Predicts with Monte Carlo method application. A C/N of 15.6 dB was considered, which is the reception threshold of the DVB-T2 standard, for 8 MHz bandwidth, modulation of 64 QAM, and code-rate of 3/4, in the Rayleigh distribution. The blue area represents 95% coverage and the yellow area represents 70% coverage. Fig. 4 shows coverage zoom in specific neighborhood.

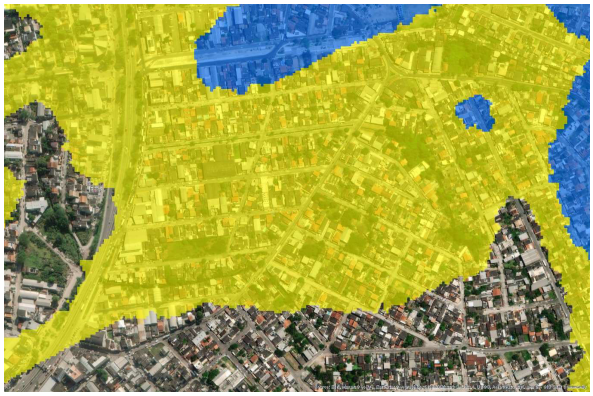

FIGURE 4. Zoom coverage area with Monte Carlo method application.

FIGURE 5. Coverage area with DCPM application.

FIGURE 6. Zoom coverage area with DCPM application.

Fig. 5 and Fig. 6 shows the same coverage simulation in the City of Rio de Janeiro, in Brazil, with the DCPM. Blue areas represents 95% coverage for the C/N of 13.7 dB for all environments, orange represents 95% coverage for the C/N of 13.5 dB for rural, hilly rural and urban environments and yellow represent 95% coverage for C/N of 13.4 dB for rural and hilly rural environments.

According to Fig. 5 and Fig. 6, the greatest probability of uncertainty is limited to a smaller area, among the possible propagation environments, considering the robustness of the communication system, under the DCPM effect. Increasing certainty implies reducing the area needed to reinforce the signal, consequently reducing the number of repeaters or the necessary transmitted signal power. The immediate consequence is an economy of both time and cost in a greener version of the broadcast system implementation.

VI. CONCLUSION

In broadcasting and long-range wireless communication systems, the main causes of uncertainty are the difficulty in representing multipath and impulsive noise because these two effects have unpredictable behavior, hard to be statistically modeled. Propagation models are available in the literature and are a statistical simplification that considers the main elements of Nature that can be minimized with uncertainty quantification algorithms.

In this article, chaotic modeling of propagation phenomena in rural, hilly rural, urban and dense urban settings was developed and tested in DVB-T2.

The DVB-T2 system has good robustness for multipath and impulsive noise. In a less robust configuration, the difference between the simpler rural environment and the complex dense urban environment is 0.3 dB. In a more robust configuration, there is no difference between the simpler rural environment and the complex dense urban environment. It can be concluded that in the DVB-T2 case, the Rayleigh distribution is too pessimistic to represent the real propagation effects.

In traditional methods of quantifying uncertainties, the algorithm shows the coverage probability of each location. Lower probability areas are considered uncertain and eligible for field measurement and coverage adjustment without in-depth analysis. The chaotic propagation model provides the worst-case reception threshold of propagation effects for each environment and transmission and reception configuration. Field measurements and coverage adjustments can improve the balance between the best case AWGN and the worst-case chaotic propagation model in each environment, reducing complexity in broadcast and long-range wireless communication systems planning.

When applying the DCPM in coverage prediction software, the uncertainty areas are limited to a smaller region, allowing the reduction of the need for field measurements to adjust the reception range and improving the designing of a communication system, considering the robustness of the modulation scheme and the propagation environment.

The DCPM can be implemented in any communication system, such as DVB-T, ATSC, ATSC3.0, and 5G mobile network.

REFERENCES

[1] J. A. J. Ribeiro, *Electromagnetic Waves Propagation, Principles and Applications*. San Jose, CA, USA: Érica Publication, Dec. 2008.
[2] P. Barsocchi, "Channel models for terrestrial wireless communications: A survey," in *Proc. Nat. Res. Council ISTI Inst.*, 2006, pp. 1–38.
[3] A. F. Molisch, *Wireless Communications*. Hoboken, NJ, USA: Wiley, 2011.
[4] B. T. Nguyen, A. Samimi, and J. J. Simpson, "A polynomial chaos approach for EM uncertainty propagation in 3D-FDTD magnetized cold plasma," in *Proc. IEEE Symp. Electromagn. Compat. Signal Integrity*, Mar. 2015, pp. 356–360, doi: 10.1109/EMCSI.2015.7107714.
[5] DVB, "Frame structure channel coding and modulation for a second generation digital terrestrial television broadcasting system (DVB-T2)," Eur. Telecommun. Standards Inst., Sophia Antipolis, France, Tech. Rep. ETSI EN 302 755, V1.4.1., 2015.
[6] V. Mohan, A. Mathur, and G. Kaddoum, "Analyzing physical-layer security of PLC systems using DCSK: A copula-based approach," *IEEE Open J. Commun. Soc.*, vol. 4, pp. 104–117, 2023, doi: 10.1109/OJCOMS.2022.3232753.
[7] V. Mohan and A. Mathur, "Secrecy analysis of DCSK-based PLC systems with multiple eavesdroppers," in *IEEE Syst. J.*, vol. 17, no. 3, pp. 3646–3657, Sep. 2023, doi: 10.1109/JSYST.2022.3224982.
[8] S. Garg, N. Sood, and C. D. Sarris, "Uncertainty quantification of ray-tracing based wireless propagation models with a control variate-polynomial chaos expansion method," in *Proc. IEEE Int. Symp. Antennas Propag. USNC/URSI Nat. Radio Sci. Meeting*, Jul. 2015, pp. 1776–1777, doi: 10.1109/APS.2015.7305277.
[9] P. Górniak, "An application of universal polynomial chaos expansion to numerical stochastic simulations of an UWB EM wave propagation," in *Proc. 11th Eur. Conf. Antennas Propag. (EUCAP)*, Mar. 2017, pp. 1878–1882, doi: 10.23919/EuCAP.2017.7928835.
[10] E. Costamagna, L. Favalli, and P. Gamba, "Multipath channel modeling with chaotic attractors," *Proc. IEEE*, vol. 90, no. 5, pp. 842–859, May 2002, doi: 10.1109/JPROC.2002.1015010.
[11] M. Hassan, U. Saeed, and W. Mahmood, "A multipath fading channel simulator based on time series generated by Lorenz chaotic attractor," in *Proc. 3rd Int. Conf. Electr. Eng.*, Apr. 2009, pp. 1–5, doi: 10.1109/ICEE.2009.5173166.
[12] B. S. Dmitriev, J. D. Zharkov, V. N. Skorokhodov, and S. A. Sadovnikov, "Ultra wide band UHF chaotic impulse generator," in *Proc. IVESC*, Apr. 2012, pp. 91–92, doi: 10.1109/IVESC.2012.6264162.
[13] N. Faruk, O. W. Bello, A. A. Oloyede, N. T. Surajudeen-Bakinde, O. Obiyemi, L. A. Olawoyin, M. Ali, and A. Jimoh, "Clutter and terrain effects on path loss in the VHF/UHF bands," *IET Microw., Antennas Propag.*, vol. 12, no. 1, pp. 69–76, Dec. 2017, doi: 10.1049/iet-map.2016.0809.
[14] V. Gonzalez-Barbone, P. Belzarena, and F. Larroca, "Software defined radio: From theory to real world communications," in *Proc. XIII Technol. Appl. Electron. Teaching Conf. (TAEE)*, Jun. 2018, pp. 1–7, doi: 10.1109/taee.2018.8476109.
[15] I. Jarin and R. Sharmin, "Performance evaluation of SISO OFDM system in the presence of CFO, timing jitter and phase noise for Rayleigh and Rician fading channels," in *Proc. IEEE Region 10 Humanitarian Technol. Conf. (R10-HTC)*, Dec. 2017, pp. 498–501, doi: 10.1109/R10-HTC.2017.8289007.
[16] C. Oestges, B. Clerckx, L. Raynaud, and D. Vanhoenacker-Janvier, "Deterministic channel modeling and performance simulation of microcellular wide-band communication systems," *IEEE Trans. Veh. Technol.*, vol. 51, no. 6, pp. 1422–1430, Nov. 2002, doi: 10.1109/TVT.2002.804846.
[17] A. Bhuvaneshwari, R. Hemalatha, and T. Satyasavithri, "Path loss prediction analysis by ray tracing approach for NLOS indoor propagation," in *Proc. Int. Conf. Signal Process. Commun. Eng. Syst.*, Jan. 2015, pp. 486–491, doi: 10.1109/SPACES.2015.7058202.
[18] N. Yee and J.-P. Linnartz, "Controlled equalization of multi-carrier CDMA in an indoor Rician fading channel," in *Proc. IEEE Veh. Technol. Conf. (VTC)*, Aug. 2002, pp. 1665–1669, doi: 10.1109/vetec.1994.345379.
[19] *Digital Mobile Land Radio Communications. Commision of the European Communities*, COST 207, Comission Eur. Communities, Brussels, Belgium, 1989.
[20] Q. H. Spencer, B. D. Jeffs, M. A. Jensen, and A. L. Swindlehurst, "Modeling the statistical time and angle of arrival characteristics of an indoor multipath channel," *IEEE J. Sel. Areas Commun.*, vol. 18, no. 3, pp. 347–360, Mar. 2000, doi: 10.1109/49.840194.
[21] J.-P. Rossi and Y. Gabillet, "A mixed ray launching/tracing method for full 3-D UHF propagation modeling and comparison with wide-band measurements," *IEEE Trans. Antennas Propag.*, vol. 50, no. 4, pp. 517–523, Apr. 2002, doi: 10.1109/tap.2002.1003388.
[22] K. Jeong, S. H. Kim, K. M. Chung, J. C. Kim, J. H. Yu, J. S. Lee, and S. H. Seo, "Multipath channel models for wireless local and metropolitan area networks," in *Proc. 3rd Int. Conf. Inf. Technol. Appl. (ICITA05)*, Aug. 2005, pp. 295–298, doi: 10.1109/icita.2005.187.

[23] A. Lipovac, S. Isak-Zatega, and P. Njemcevic, "In-service testing OFDM error floor by constellation analysis," in *Proc. 25th Int. Conf. Softw., Telecommun. Comput. Netw. (SoftCOM)*, Sep. 2017, pp. 1–5, doi: 10.23919/SOFTCOM.2017.8115549.
[24] J.-H. Yan, J.-S. Tseng, S.-C. Tsai, and K.-M. Feng, "A neural network based joint CFO-SCO equalization for OFDM-RoF in multi-band mobile fronthaul," in *Proc. Opto-Electron. Commun. Conf. (OECC)*, Oct. 2020, pp. 1–3, doi: 10.1109/OECC48412.2020.9273585.
[25] M. Krondorf, T.-J. Liang, and G. Fettweis, "Symbol error rate of OFDM systems with carrier frequency offset and channel estimation error in frequency selective fading channels," in *Proc. IEEE Int. Conf. Commun.*, Jun. 2007, pp. 5132–5136, doi: 10.1109/icc.2007.848.
[26] J. Zhang and Z. Zhang, "Simulation and analysis of OFDM system based on Simulink," in *Proc. Int. Conf. Commun., Circuits Syst. (ICCCAS)*, Jul. 2010, pp. 28–31, doi: 10.1109/ICCCAS.2010.5582049.
[27] G. Bedicks, F. Yamada, F. Sukys, C. E. S. Dantas, L. T. M. Raunheitte, and C. Akamine, "Results of the ISDB-T system tests, as part of digital TV study carried out in Brazil," *IEEE Trans. Broadcast.*, vol. 52, no. 1, pp. 38–44, Mar. 2006, doi: 10.1109/TBC.2005.856729.
[28] T. S. Rappaport, *Wireless Communications: Principles and Practice*, 2nd ed. Upper Saddle River, NJ, USA: Prentice-Hall, Jan. 2002.
[29] P. Pedrosa, R. Dinis, and F. Nunes, "Iterative frequency domain equalization and carrier synchronization for multi-resolution constellations," *IEEE Trans. Broadcast.*, vol. 56, no. 4, pp. 551–557, Dec. 2010, doi: 10.1109/TBC.2010.2073251.
[30] Z. Wang, Y. Xin, G. Mathew, and X. Wang, "Efficient phase-error suppression for multiband OFDM-based UWB systems," *IEEE Trans. Veh. Technol.*, vol. 59, no. 2, pp. 766–778, Feb. 2010, doi: 10.1109/TVT.2009.2035324.
[31] E. J. Marchi, M. A. Cervetto, and M. L. Tenorio, "A DDR3 memory based time interleaving FPGA implementation for ISDB-T standard," in *Proc. 7th Southern Conf. Program. Log. (SPL)*, Apr. 2011, pp. 1–5, doi: 10.1109/SPL.2011.5782616.
[32] D. Middleton, "Non-Gaussian noise models in signal processing for telecommunications: New methods an results for class A and class B noise models," *IEEE Trans. Inf. Theory*, vol. 45, no. 4, pp. 1129–1149, May 1999, doi: 10.1109/18.761256.
[33] H. N. Abdul, K. Rajani, and K. V. Padmaja, "BER performance of BPSK and QPSK over Rayleigh channel and AWGN channel," *Int. J. Eletrical Electron. Eng. Telecommun.*, vol. 3, no. 2, pp. 12–16, Apr. 2014. [Online]. Available: http://www.ijeetc.com/index.php?m=content&c=index&a=show&catid=154&id=889
[34] M. G. Sanchez, L. de Haro, M. C. Ramon, A. Mansilla, C. M. Ortega, and D. Oliver, "Impulsive noise measurements and characterization in a UHF digital TV channel," *IEEE Trans. Electromagn. Compat.*, vol. 41, no. 2, pp. 124–136, May 1999, doi: 10.1109/15.765101.
[35] G. A. Tsihrintzis and C. L. Nikias, "Fast estimation of the parameters of alpha-stable impulsive interference," *IEEE Trans. Signal Process.*, vol. 44, no. 6, pp. 1492–1503, Jun. 1996, doi: 10.1109/78.506614.
[36] M. Ghosh, "Analysis of the effect of impulse noise on multicarrier and single carrier QAM systems," *IEEE Trans. Commun.*, vol. 44, no. 2, pp. 145–147, Feb. 1996, doi: 10.1109/26.486604.
[37] J. Lago-Fernández and J. Salter, "Modelling impulsive interference in DVB-T," EBU, Grand-Saconnex, Switzerland, Tech. Rev., White Paper WHP 080, Jul. 2004.
[38] G. Bedicks, C. E. S. Dantas, F. Sukys, F. Yamada, L. T. M. Raunheitte, and C. Akamine, "Digital signal disturbed by impulsive noise," *IEEE Trans. Broadcast.*, vol. 51, no. 3, pp. 322–328, Sep. 2005, doi: 10.1109/tbc.2005.851139.
[39] A. Wagstaff and N. Merricks, "Man-made noise measurement programme," *IEE Proc. Commun.*, vol. 152, no. 3, p. 371, Jun. 2005, doi: 10.1049/ip-com:20045025.
[40] A. Chandra, "Measurements of radio impulsive noise from various sources in an indoor environment at 900 MHz and 1800 MHz," in *Proc. 13th IEEE Int. Symp. Pers., Indoor Mobile Radio Commun.*, Dec. 2002, pp. 639–643, doi: 10.1109/pimrc.2002.1047300.
[41] P. Torio and M. G. Sanchez, "Mitigation of impulsive noise in digital video broadcasting terrestrial using orthogonal polarization reception," *IEEE Trans. Consum. Electron.*, vol. 55, no. 4, pp. 1798–1804, Nov. 2009, doi: 10.1109/TCE.2009.5373734.
[42] B. Arambepola, "Method of and apparatus for detecting impulsive noise, method detecting impulsive noise, method of operating a demodulator, demodulator and radio receiver," United States Patent 7 302 024B2, Nov. 27, 2007.
[43] A. Mengi and A. J. H. Vinck, "Successive impulsive noise suppression in OFDM," in *Proc. ISPLC*, Mar. 2010, pp. 33–37, doi: 10.1109/ISPLC.2010.5479927.
[44] D. F. Drake and D. B. Williams, "Linear, random representations of chaos," *IEEE Trans. Signal Process.*, vol. 55, no. 4, pp. 1379–1389, Apr. 2007, doi: 10.1109/tsp.2006.888885.
[45] M. Eisencraft, "Discrete-time chaos: Introduction, examples and statistical representation," *J. Brazilian Soc. Comput. Intell.*, vol. 16, no. 1, pp. 1–25, Dec. 2017, doi: 10.13140/RG.2.2.36205.90083.
[46] R. Devaney, *An Introduction To Chaotic Dynamical Systems*. San Francisco, CA, USA: Benjamin/Cummings, 1986.
[47] S. H. Strogatz, *Nonlinear Dynamics and Chaos*. Boston, MA, USA: Addison-Wesley, 1994.
[48] D. M. Kato, "Spectral analysis of chaotic signals generated by one-dimensional maps," MSc dissertation, Universidade Presbiteriana Mackenzie, São Paulo, Brazil, 2008.
[49] M. Hénon, "A two-dimensional mapping with a strange attractor," *Commun. Math. Phys.*, vol. 50, no. 1, pp. 69–77, Feb. 1976.
[50] O. Haffenden, "DVB-T2: The common simulation platform," Brit. Broadcast. Corp. Res., London, U.K., White Paper WHP 196, May 2011.
[51] DVB, "Implementation guidelines for a second generation digital terrestrial television broadcasting system (DVB-T2)," Eur. Telecommun. Standards Inst., Sophia Antipolis, France, Tech. Rep. ETSI TS 102 831, V1.2.1, Aug. 2012.
[52] *Progira*. Accessed: Sep. 2023. [Online]. Available: https://www.progira.com
[53] *ArcGis*. Accessed: Sep. 2023. [Online]. Available: https://www.esri.com/en-us/arcgis/about-arcgis/overview

ALBERTO LEONARDO PENTEADO BOTELHO received the degree in electrical engineering from Universidade Paulista (UNIP), the Engineering degree specialized in digital television systems from Instituto Nacional de Telecomunicações (Inatel), the Engineering degree in telecommunications networks from Inatel, the M.B.A. degree in project management from Fundação Getúlio Vargas (FGV), and the Master of Science degree in electrical engineering from Universidade Presbiteriana Mackenzie, where he is currently pursuing the Ph.D. degree in electrical engineering. He was with Rede TV!, from 2002 to 2011. Since 2011, he has been with LM Telecom as a Project Engineer, where he has had the opportunity to work with broadcast network.

CRISTIANO AKAMINE received the B.Sc. degree in electrical engineering from Mackenzie Presbyterian University, São Paulo, Brazil, in 1999, and the M.Sc. and Ph.D. degrees in electrical engineering from the State University of Campinas (UNICAMP), São Paulo, in 2004 and 2011, respectively. He is currently a Professor in embedded systems, software defined radio and advanced communication with Mackenzie Presbyterian University. He has been a Researcher with the Digital TV Research Laboratory, Mackenzie Presbyterian University, since 1998, where he has had the opportunity to work with many digital TV systems. His research interests include a system on chip for broadcast TV and software defined radio.

PAULO BATISTA LOPES received the B.Sc. and M.Sc. degrees in EE from the Federal University of Rio de Janeiro, Brazil, in 1978 and 1981, respectively, and the Ph.D. degree in EE from Concordia University, Montreal, Canada, in 1985. From 1985 to 1988, he was with Elebra and CMA, two Brazilian companies, working on the design of several communication equipments. From 1988 to 1999, he was with Texas Instruments as a DSP Specialist. In 1999, he moved to Motorola-SPS (later to become Freescale Semiconductor) as a Sales and Application Manager. Since 2009, he has been a Professor with the School of Engineering, Mackenzie Presbyterian University. His research interests include circuit theory, digital signal processing, analog circuit design and communication theory, and the Internet of Things.